REPORT DOCUMENTATION PAGE

Public reporting burden for this collection of information is estimated to average 1 hour per response, including the time for reviewing instructions, searching existing data sources, gathering and maintaining the data needed, and completing and reviewing this collection of information. Send comments regarding this burden estimate or any other aspect of this collection of information, including suggestions for reducing this burden to Department of Defense, Washington Headquarters Services, Directorate for Information Operations and Reports (0704-0188), 1215 Jefferson Davis Highway, Suite 1204, Arlington, VA 22202-4302. Respondents should be aware that notwithstanding any other provision of law, no person shall be subject to any penalty for failing to comply with a collection of information if it does not display a currently valid OMB control number. **PLEASE DO NOT RETURN YOUR FORM TO THE ABOVE ADDRESS.**

1. REPORT DATE *(DD-MM-YYYY)* 2010	2. REPORT TYPE open literature publication	3. DATES COVERED *(From - To)*

4. TITLE AND SUBTITLE Sulfur mustard induced cytokine production and cell death: Investigating the potential roles of the p38, p53, and NF-kappaB signaling pathways with RNA interference	5a. CONTRACT NUMBER
	5b. GRANT NUMBER
	5c. PROGRAM ELEMENT NUMBER
6. AUTHOR(S) Ruff, AL and Dillman, JF III	5d. PROJECT NUMBER
	5e. TASK NUMBER
	5f. WORK UNIT NUMBER

7. PERFORMING ORGANIZATION NAME(S) AND ADDRESS(ES) US Army Medical Research Institute of Chemical Defense ATTN: MCMR-CDR-C 3100 Ricketts Point Road Aberdeen Proving Ground, MD 21010-5400	8. PERFORMING ORGANIZATION REPORT NUMBER USAMRICD-P08-012

9. SPONSORING / MONITORING AGENCY NAME(S) AND ADDRESS(ES) US Army Medical Research Institute of Institute of Chemical Defense ATTN: MCMR-CDZ-P 3100 Ricketts Point Road Aberdeen Proving Ground, MD 21010-5400	10. SPONSOR/MONITOR'S ACRONYM(S)
	11. SPONSOR/MONITOR'S REPORT NUMBER(S)

12. DISTRIBUTION / AVAILABILITY STATEMENT

Approved for public release; distribution unlimited

13. SUPPLEMENTARY NOTES
Published in Journal of Biochemical and Molecular Toxicology, 24(3), 155-164, 2010. Grant Sponsor: Defense Threat Reduction Agency—Joint Science and Technology Office, Medical S&T Division.

14. ABSTRACT
See reprint

15. SUBJECT TERMS
Sulfur mustard; Inflammation; p38MAPK; NF-κB; p53; Cell death

16. SECURITY CLASSIFICATION OF:			17. LIMITATION OF ABSTRACT	18. NUMBER OF PAGES	19a. NAME OF RESPONSIBLE PERSON James F. Dillman III
a. REPORT UNLIMITED	b. ABSTRACT UNLIMITED	c. THIS PAGE UNLIMITED	UNLIMITED	11	19b. TELEPHONE NUMBER *(include area code)* 410-436-1723

Sulfur Mustard Induced Cytokine Production and Cell Death: Investigating the Potential Roles of the p38, p53, and NF-κB Signaling Pathways with RNA Interference

Albert L. Ruff and James F. Dillman III

Cell and Molecular Biology Branch, Research Division, U.S. Army Medical Research Institute of Chemical Defense, 3100 Ricketts Point Road, Aberdeen Proving Ground, MD 21010–5400, USA; E-mail: *james.dillman@us.army.mil*

ABSTRACT: Cutaneous and ocular injuries caused by sulfur mustard (SM; bis-(2-chloroethyl) sulfide) are characterized by severe inflammation and death of exposed cells. Given the known roles of p38MAPK and NF-κB in inflammatory cytokine production, and the known roles of NF-κB and p53 in cell fate, these pathways are of particular interest in the study of SM injury. In this study, we utilized inhibitory RNA (RNAi) targeted against p38α, the p50 subunit of NF-κB, or p53 to characterize their role in SM-induced inflammation and cell death in normal human epidermal keratinocytes (NHEK). Analysis of culture supernatant from 200 μM SM-exposed cells showed that inflammatory cytokine production was inhibited by p38α RNAi but not by NF-κB p50 RNAi. These findings further support a critical role for p38 in SM-induced inflammatory cytokine production in NHEK and suggest that NF-κB may not play a role in the SM-induced inflammatory response of this cell type. Inhibition of NF-κB by p50 RNAi did, however, partially inhibit SM-induced cell death, suggesting a role for NF-κB in SM-induced apoptosis or necrosis. Interestingly, inhibition of p53 by RNAi potentiated SM-induced cell death, suggesting that the role of p53 in SM injury, may be complex and not simply prodeath. © 2010 Wiley Periodicals, Inc. J Biochem Mol Toxicol 00:1–10, 2010; Published online in Wiley InterScience (www.interscience.wiley.com). DOI 10.1002/jbt.20321

INTRODUCTION

Sulfur mustard (SM; bis-(2-chloroethyl) sulfide) is a highly reactive bifunctional alkylating agent that covalently modifies DNA, protein, and other biological molecules. This compound is potently toxic and has been used as a vesicant in military campaigns since the First World War. Skin is a major target tissue, and clinical presentations of SM cutaneous injuries are characterized by vesication and severe inflammation [1]. The molecular mechanisms that lead to these signs and symptoms are not well understood; however, the known roles of p38 [2,3], p53 [4], and NF-κB [5] in cell physiology have made these pathways of particular interest in the study of the cellular response to SM.

Inflammatory cytokines shown to be induced by SM, IL-1β, IL-6, IL-8, and TNFα [6–8], are known to be modulated by p38 and/or NF-κB in other systems [3,5]. Both p38 and NF-κB are activated in SM-exposed cells [7,9–11], but it is NF-κB that has long been implicated as playing a primary role in SM-induced inflammatory cytokine production [9,12–14]. These implications have been based on the observations that (1) SM- or SM analog-induced modulation of NF-κB activity in gel shift assays correlates with inflammatory or protection events, and (2) NF-κB exhibits proinflammatory activity in other systems [15,16]. Less has been reported regarding the role of p38 in SM injury. A previous study by our laboratory showed that SB203580, a small molecule inhibitor of p38, substantially and significantly decreased inflammatory cytokine production [7]. This suggests that p38 may play a more critical

The opinions or assertions contained herein are the private views of the authors and are not to be construed as official or as reflecting the views of the Department of the Army or the Department of Defense.

role than NF-κB in SM-induced inflammatory cytokine production. However, experiments that would more clearly define the roles of p38 and NF-κB in SM-induced cytokine production and inflammation have not been published.

Another characteristic of SM cutaneous injury is extensive death of basal keratinocytes [17,18]. This presents another possible role for NF-κB in SM injury since NF-κB is known to play a role in cell fate following injury or stress in other systems [19–22]. However, p53 is also activated in SM injury [10,23–25]. Given that SM is known to damage DNA and the classical role of p53 is in cell cycle arrest and apoptosis, p53 has been widely implicated in SM-induced cell death [10,23,24,26,27].

Although p38, p53, and NF-κB have been implicated in the response of cells to SM, the roles of these major pathways in SM injury remain unclear. To further our understanding of these molecules in SM injury, we have surveyed the effects of RNAi against p38α, p53, and NF-κB1 (the p50 subunit of NF-κB) on SM-induced inflammation, cell death, and phenotypic changes in normal human epidermal keratinocytes (NHEK).

MATERIALS AND METHODS

Cell Culture

NHEK were obtained as cryopreserved stocks from Cascade Biologics (a division of Invitrogen, Carlsbad, CA). All studies included the use of NHEK from two different donors. Cells were seeded at 2.5×10^3 cells/cm^2 into 75 cm^2 flasks. Cells were grown in serum-free supplemented keratinocyte growth medium (EpiLife, Cascade Biologics) to 80%–90% density prior to passaging and reseeding at 2.5×10^3 cells/cm^2 into T-25 flasks, 6-well plates, or 24-well plates. The cells were grown at 37°C with 5% CO$_2$. Second and third passages postcryopreserved seedings were used for exposures at 80%–90% confluence.

RNAi Transfection

Target genes p38α, p53, and NF-κB1 (the p50 subunit of NF-κB) were silenced using Validated Stealth RNAi DuoPaks (Invitrogen). Each target was silenced using a mixture of both sequences from the DuoPak in equal molar amounts. Lipofectamine RNAiMAX transfection reagent (Invitrogen) was used to transfect the RNAi. RNAi and transfection reagent were diluted in Opti-MEM reduced-serum medium (Invitrogen), mixed, and then added to cells. Cells were transfected for 6 h, then washed with phosphate buffered saline (PBS, 10 mM sodium phosphate, 0.9% NaCl, pH 7.4) and overlaid with fresh culture medium. To achieve

equivalent RNAi transfection across different types of culture vessels (T-25, 6-well, and 24-well plates), RNAi was administered to the cells relative to the area of the culture vessel. This method gave equivalent target knockdown across different culture vessels (data not shown). Transfection optimization studies were performed for each target to determine the minimal dose necessary to achieve at least 70% knockdown as determined by Western blot analysis. It was determined that 4 pmol/cm^2 for p38α and 6 pmol/cm^2 for p53 and NF-κB1 were optimal at a ratio of 1 μL RNAi (20 μM) to 1.5 μL transfection reagent.

RNAi Target Specificity Controls

Validated Stealth Negative Control Duplex RNAi was utilized to control for off-target effects. The duplex was configured to match the guanine cytosine (GC) content of the targeting RNAi and transfected as described above. For each target described above, one sequence had low GC content (35%–45%) and the other had medium GC content (45%–55%). The negative control consisted of a mixture of one sequence with low GC content (36%) and one medium GC content (48%) in equal molar amounts. Results with p38α RNAi were confirmed by comparison to control SM exposures of NHEK treated with 10 μM of SB203580 (or DMSO vehicle control) as described previously [7]. Highly specific small molecule inhibitors are not available for p53 and NF-κB1. Therefore, target specific effects for these molecules were confirmed by testing the two RNAi sequences in each DuoPak independently. Each sequence tested at the same concentration as the duplex (6 pmol/cm^2).

SM Exposures

SM was obtained from the U.S. Army Edgewood Chemical Biological Center (Aberdeen Proving Ground, MD). All SM exposures were performed in a certified chemical surety fume hood. A frozen aliquot of neat (undiluted) SM in keratinocyte growth medium was thawed and vortexed to generate a 4-mM SM stock solution. This stock solution was placed on ice and immediately diluted into medium to expose cells to SM. The exposure dose was 200 μM SM for all experiments. Cells were maintained at 37°C with 5% CO$_2$ during pretreatments. For SM exposures, cells were left at 37°C with room CO$_2$ concentrations for a maximum of 30 min and returned to 37°C with 5% CO$_2$ for the remainder of the postexposure time period.

Membrane Integrity Assay

Lactate dehydrogenase (LDH) activity in cell medium was used as a correlate of membrane integrity

and cell viability [28,29] and measured with the CytoTox-ONE Homogeneous Membrane Integrity Assay Kit (Promega, Madison, WI). Culture medium was collected to measure spontaneous release of LDH, and cells were lysed for total LDH. Samples were transferred to a 96-well black plate and mixed with an equal volume of assay buffer. After 10 min of incubation at room temperature, stop solution was added to each well. Fluorescence was recorded with a Genios (TECAN US, Research Triangle Park, NC) plate reader equipped with a 535-nm excitation wavelength filter and a 595-nm emission filter. The data are expressed as the percent membrane integrity over time (average of three biological replicates ± standard error (SD)). Each biological replicate was analyzed in triplicate (three technical replicates for each biological replicate).

Cytokine Analysis

The levels of cytokines in culture medium samples were measured using the Beadlyte Human Multi-Cytokine Detection System 2 (Millipore, Billerica, MA). Culture medium was removed from each vessel and immediately stored at $-80°C$ for subsequent analysis. The samples were briefly centrifuged in a refrigerated microfuge to remove cellular debris. The assay was performed according to the manufacturer's instructions and analyzed using a Bio-Plex System array reader with Bio-Plex Manager 4.0 software (Bio-Rad Laboratories, Hercules, CA). The data are expressed as the average of the number of biological replicates ± standard deviation (SD). Each biological replicate was a separate plating, and each biological replicate was analyzed in triplicate (three technical replicates for each biological replicate).

Isolation of Proteins and Gel Electrophoresis

The culture medium was removed from the cells, and the cells were washed with PBS. The cells were lysed with 350 μL SDS lysis buffer (125 mM Tris, 4% SDS, 20% glycerol, pH 6.8), scraped from the culture vessel, and collected into 0.5 mL tubes containing 100 μL of 0.5 mm glass beads. The lysates were then homogenized at 4°C for 30 s in a mini-bead beater (BioSpec Products Inc., Bartlesville, OK). SM exposure has been shown to induce changes in the expression of housekeeping genes, making normalization to a housekeeping gene inaccurate [26]. To address this issue, we normalized to total protein content by precisely quantifying the amount of total protein in each sample using the EZQ Protein Quantitation kit (Invitrogen) prior to gel loading. The samples were then resolved on 10% criterion precast Bis-Tris SDS polyacrylamide gels (BioRad, Hercules, CA) with 50 μg of protein loaded per lane.

Immunoblotting

Resolved proteins were transferred from polyacrylamide gels to polyvinylidene fluoride membranes (PVDF; Hybond, Amersham Pharmacia Biotech, Piscataway, NJ) by electroblotting. The membranes were blocked with 5% nonfat dry milk in TBST (60 mM Tris, pH 7.5, 0.9% sodium chloride, 0.1% Tween 20). The blots were probed with primary antibodies diluted in 5% bovine serum albumin (Sigma Aldrich, St. Louis, MO). All primary antibodies were obtained from Cell Signaling Technology (Beverly, MA) and diluted 1:2000 in blocking buffer for blotting. Primary antibodies were rabbit polyclonal phospho-p53 (ser 15) antibody (Cat# 9284), rabbit polyclonal p53 antibody (Cat# 9282), rabbit polyclonal IκBα antibody (Cat# 9242), rabbit polyclonal p38α antibody (Cat# 9218), rabbit polyclonal NF-κB1 p105/p50 antibody (Cat# 3035), mouse monoclonal antibody phospho-p38 MAPK antibody (Thr180/Tyr182) (Cat#9216), and rabbit polyclonal p38 antibody (Cat# 9212). Primary antibody was detected via an alkaline phosphatase conjugated mouse antirabbit secondary antibody (Zymed Laboratories, Invitrogen) and enhanced chemifluorescence (ECF; Amersham Pharmacia Biotech, Piscataway, NJ). The fluorescent signal was detected and visualized using a Typhoon scanner (Molecular Dynamics, Sunnyvale, CA) and analyzed using ImageQuant software Version II (Molecular Dynamics).

Statistical Analyses

Cytokine production in pg/mL is expressed as the average ± SD ($n = 5$ for p53 and NF-κB1 RNAi groups, $n = 6$ for p38α groups, and $n = 8$ for all other groups). The percent loss of membrane integrity is expressed as the mean ± SD ($n = 3$). Data were analyzed for statistical significance using a one-way analysis of variance (ANOVA) followed by Bonferonni's multiple comparison tests.

Microscopy

Digital image microscopy was performed using an Olympus CKX41 culture microscope (WHB10X eyepiece with a 10 × objective) and DP12 microscope digital camera system (Olympus America, Inc., Melville, NY). Images were compiled using Adobe Photoshop Elements version 6.0 (San Jose, CA).

RESULTS

Target Knockdown by RNAi

We investigated p38, p53, and NF-κB to clarify their roles in the cellular response to SM injury. We utilized RNAi for target inhibition because, relative to many pharmacologic inhibitors, RNAi has greater target specificity, and negative controls can be employed. RNAi targeting p38α was chosen because it is the major p38 isoform involved in the immune response and inflammatory cytokine production [30] and the major p38 isoform in NHEK (data not shown). Our intent for NF-κB was to assess the role of the classical activation pathway in cytokine production in SM-exposed NHEK. Although there are some exceptions, the classical NF-κB activation pathway with the p50–p65 heterodimer is implicated in the NF-κB-driven expression of the inflammatory cytokines of interest in this study [5,31]. Our selection of p50 was based on this data that inhibition of p50 should interfere with NF-κB-driven expression of genes in response to SM. This is consistent with the finding of Rebholz et al. that the canonical NF-kB pathway is involved in the response to SM [11].

To assess and confirm target knockdown by RNAi, target expression was evaluated by Western blot analysis (Figure 1). Western blot densitometry analysis showed that RNAi knocked down p38α protein expression 89% relative to the average of the naïve and control RNAi-treated cells. Western blot analysis for total p38 showed that p38α RNAi knocked down total p38 expression 79% (data not shown). These results suggest that p38α is the major isoform of p38 in NHEK, comprising approximately 90% of the total p38 in the cell. Western blot densitometry analysis showed that p50, p105, and p53 expression was knocked down 78%, 82%, and 92%, respectively. These data also show that knock down of any one of the proteins of interest (p38α, p53,

NF-κB1) did not alter the expression levels of the other targets. Knockdown of p50, p105, and p53 expression by the independent sequences of the NF-κB1 and p53 duplexes RNAi was within 10% of the expression levels described above (data not shown).
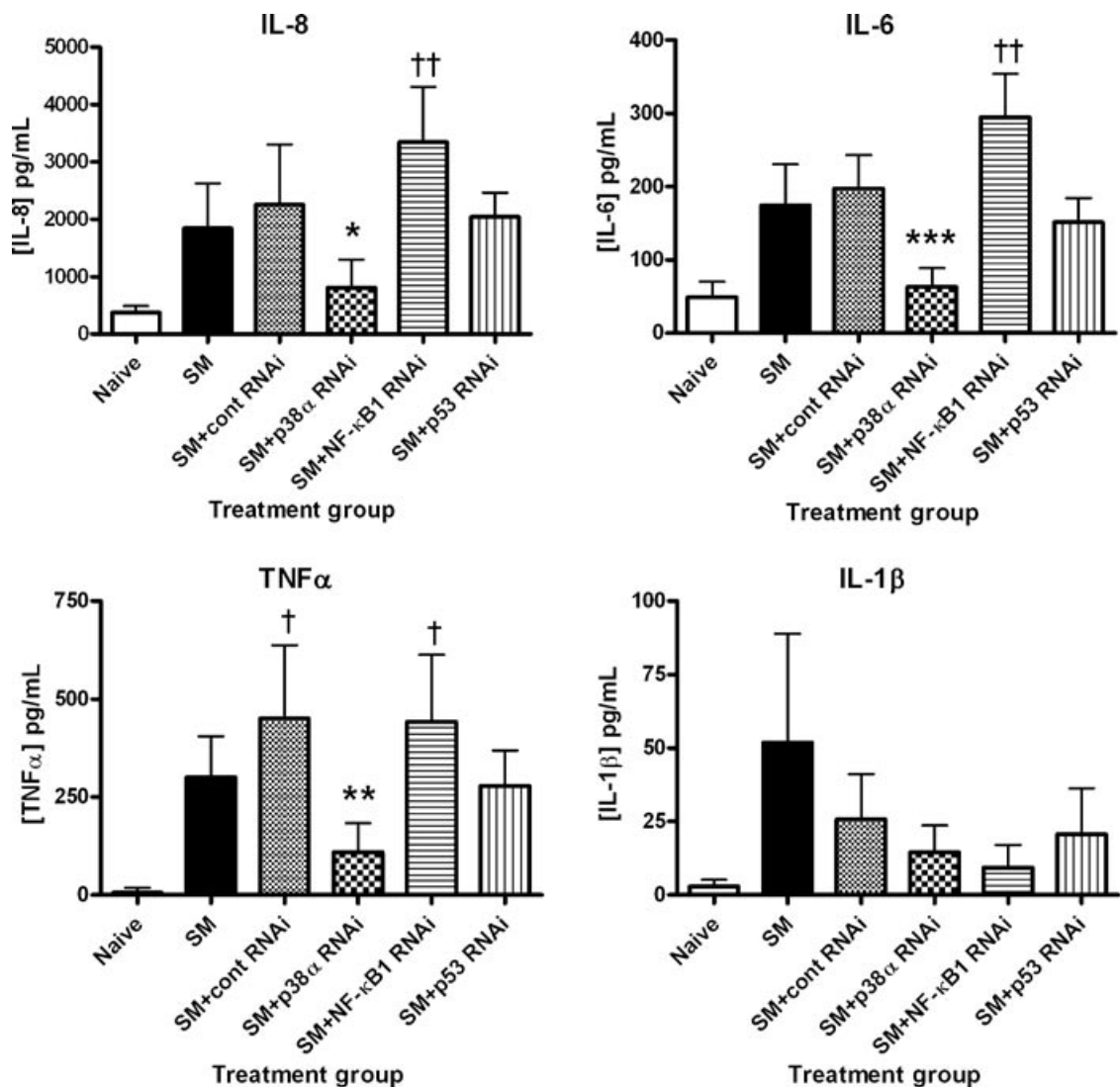
Inflammatory Cytokine Production

NHEK were treated with RNAi and exposed to 200 μM SM. Inflammatory cytokines secreted by NHEK into the culture medium were measured 24 h after exposure. Production of cytokines by unexposed RNAi-treated NHEK was similar to naïve cells (data not shown). SM exposure induced NHEK to produce IL-8, IL-6, TNFα, and IL-1β (Figure 2). p38α RNAi was the only treatment that inhibited the production of IL-8, IL-6, and TNFα. This inhibition was significant relative to both the SM and SM control RNAi groups. SB203580 produced the same effects as p38α RNAi with the exception that cytokine inhibition was generally greater with SB203580 (data not shown). NF-κB1 RNAi did not inhibit the SM-induced production of these cytokines, but rather significantly elevated the production of IL-8 and IL-6 relative to the SM group. Similar results were obtained with each of the NF-κB1 RNAi DuoPak sequences when tested separately (data not shown). The production of IL-8, IL-6, and TNFα by p53 RNAi-treated SM-exposed cells was equivalent with the SM group and not significantly different from the SM-exposed control RNAi group, which had slightly elevated levels of these cytokines. Similar results were obtained with each of the p53 RNAi duplex sequences when tested separately (data not shown). All RNAi treatment groups significantly decreased the production of IL-1β by SM-exposed cells to about half the level of the SM group. Further inhibition of SM-induced production of IL-1β was observed with p38α and NF-κB1 RNAi treatment; however, neither was significant relative to the SM-exposed control RNAi group. IL-1β production by SM-exposed p53 RNAi-treated cells was similar to that of SM-exposed control RNAi-treated cells.
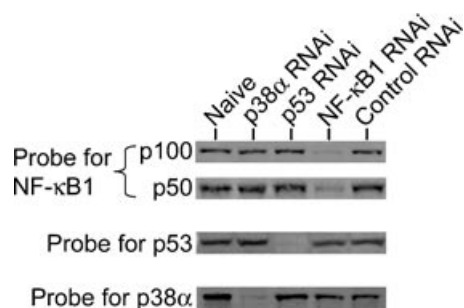
FIGURE 1. Western blot analysis of p38α, p53, and p50/p100 (NF-κB1) knockdown by RNAi in NHEK. NHEK were treated with p38α, p53, NF-κB1, or control RNAi, and whole cell lysates were prepared 48 h after transfection. Samples were resolved by SDS PAGE, immunoblotted, and probed with an antibody for each target. The data shown are representative of three biological replicates.

Cell Viability and Cell Morphology

LDH activity in cell medium was used as a correlate of membrane integrity and cell viability. NHEK were treated with RNAi and exposed to 200 μM SM; LDH in cell medium was then assayed at 1, 2, 4, 8, and 24 h after exposure. Membrane integrity of all unexposed RNAi-treated NHEK was similar to naïve cells at all time points, with the exception of unexposed p53 RNAi-treated cells, which was 1%–2% lower at each time point. SM exposure induces only a small

FIGURE 2. Analysis of inflammatory cytokines IL-6, IL-8, TNFα, and IL-1β in culture medium from RNAi-treated SM-exposed NHEK. NHEK were treated with RNAi for 48 h and exposed to 200 μM SM. Culture medium was collected 24 h postexposure and briefly centrifuged prior to multiplex assay for inflammatory cytokines. Each biological replicate was a separate plating, and each was analyzed in triplicate (three technical replicates for each biological replicate). The data are expressed as pg/mL of the average ± SD ($n = 5$ for p53 and NF-κB1 RNAi groups, $n = 6$ for p38α RNAi groups, and $n = 8$ all other groups). Cytokine production significantly less than the SM-exposed group and SM-exposed control RNAi-treated group is indicated by asterisks ($^*p < 0.05$, $^{**}p < 0.01$, $^{***}p < 0.001$). Cytokine production significantly greater than the SM-exposed group is indicated by symbol †($^†p < 0.05$, $^{††}p < 0.001$).

loss in membrane integrity at early time points, which is first observable at 4 h after exposure (Figure 3). At 24 h after exposure, the loss of membrane integrity is greater. Treatment with p38α or control RNAi does not adversely affect nor improve the membrane integrity of exposed cells at 0–8 h. However, the membrane integrity of these groups at 24 h was slightly less, presumably due to transfection-related stress. Treatment with p53 RNAi significantly accelerated and potentiated the SM-induced loss of membrane integrity. This loss was first observable just 4 h after exposure and significantly greater than in all other experimental groups
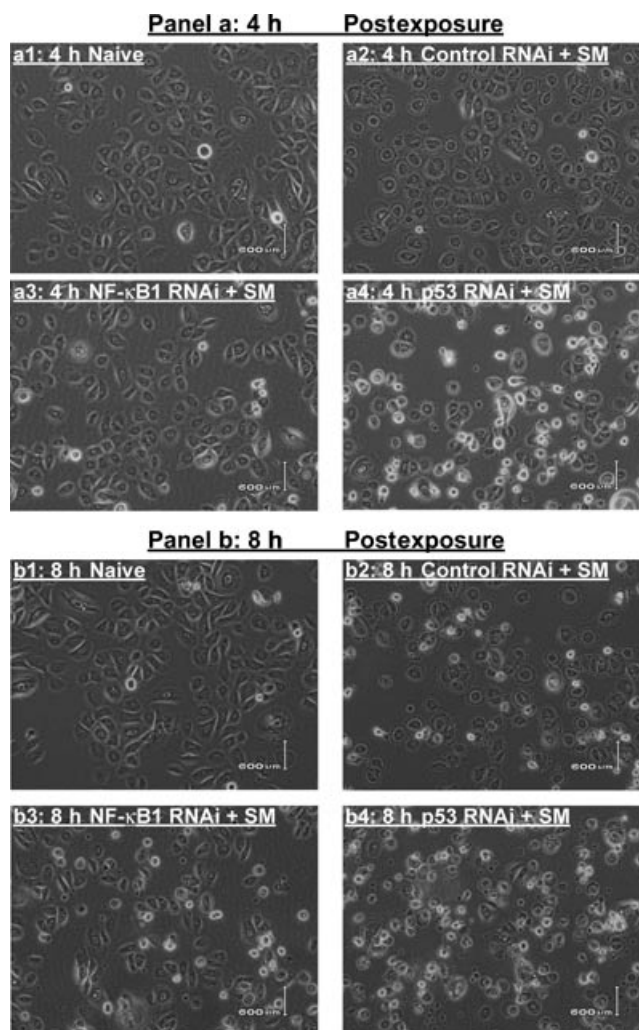
at the 8- and 24-h time points. SM-exposed NF-κB1 RNAi-treated cells had modest, but significantly better, membrane integrity than did all other SM-exposed groups at the 24-h time point.

The effects of RNAi treatment on the SM-induced loss of membrane integrity correlated with SM-induced changes in cell morphology observed by microscopy. It should be noted that any possible relationship between early phenotypic changes and ultimate death by necrosis has not been established. Thus, the assessment of general cell health by phenotypic appearance and assessment of necrosis by LDH release are
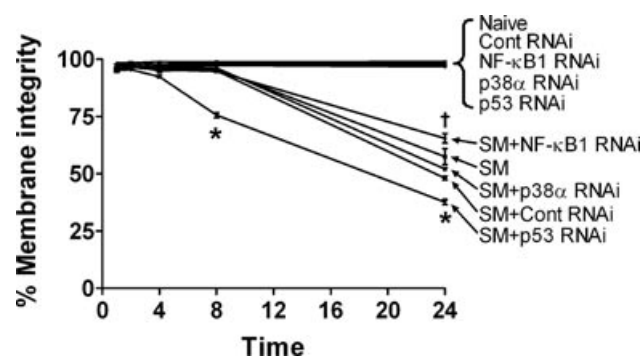
FIGURE 3. Analysis of membrane integrity by LDH assay. LDH activity in cell medium was used as an indicator of membrane integrity. NHEK were treated with RNAi for 48 h and exposed to 200 μM SM for 24 h. Culture medium was collected to measure spontaneous release of LDH, and cells were lysed for total LDH. LDH release was assessed at 1, 2, 4, 8, and 24 h post-SM exposure. The data are expressed as percent membrane integrity over time of the average of three biological replicates ± SD. Each biological replicate was analyzed in triplicate (three technical replicates for each biological replicate). Membrane integrity significantly less than all SM-exposed groups is indicated by asterisks ($p < 0.001$). Membrane integrity significantly greater than all SM-exposed groups is indicated by symbol †($p < 0.001$).

FIGURE 4. Phase contrast photomicrographs of SM-exposed NHEK 4 h (panel a) and 8 h (panel b) postexposure. NHEK were treated with RNAi for 48 h and exposed to 200 μM SM for the indicated time points. Cells were then evaluated by phase contrast microscopy using an Olympus CKX41 microscope. Photomicrographs were captured with an Olympus DP12 camera. Micrographs are representative of three biological replicates.

complimentary, but not necessarily related, analyses. Photomicrographs of naïve cells and SM-exposed cells that have been treated with control, NF-κB1, or p53 RNAi at 4 h postexposure are shown in Figure 4 (panel a). The morphology changes seen in the SM-exposed control RNAi group (Figure 4, panel a2) are representative of the SM-exposed cells, SM-exposed p38α RNAi-treated cells, SM-exposed SB203580-treated cells, and SM-exposed DMSO vehicle control cells (data not shown). The edges of virtually all the cells have a jagged appearance possibly due to early events of cell detachment related to condensation. In contrast, the SM-exposed NF-κB1 RNAi-treated cells (Figure 4, panel a3) had very smooth edges and were virtually indistinguishable from naïve cells (Figure 4, panel a1) at the 4-h point. At 8 h, SM-exposed NF-κB1 RNAi-treated cells (Figure 4, panel b3) have a larger fraction of detached cells relative to the 4-h time point, but those that remained attached looked very similar to naïve cells (Figure 4, panel b1). Similar results were obtained with each of the independently tested NF-κB1 RNAi duplex sequences (data not shown). The most pronounced SM-induced changes in cell morphology were seen in the SM-exposed p53 RNAi group. At just 4 h, the majority of these cells were condensed, and those that remained attached to the culture flask had jagged edges (Figure 4, panel a4). At 8 h after SM exposure, virtually all the cells in the SM-exposed p53 RNAi group were condensed (Figure 4, panel b4). In contrast, most cells in the 8-h SM-exposed control RNAi group (Figure 4, panel b2) remained attached, and only a fraction of the cells had

condensed. The 8-h SM exposed p53 RNAi group appeared most similar to the 24-h SM group in which the majority of the cells had condensed (see supplemental data). Similar results were obtained with each of the independently tested p53 RNAi duplex sequences (data not shown). At 24 h postexposure, there appeared to be extensive cell death (cell condensation) in all the SM-exposed groups and virtually no difference in cell morphology between any of the SM-exposed treatment groups at this time point (see panel c of Figure 4 in supplemental data). Thus, the modest improvement in membrane integrity of NF-κB1 RNAi-treated cells seen by LDH assay was not observable by cell morphology. None of the SM-induced morphology changes were
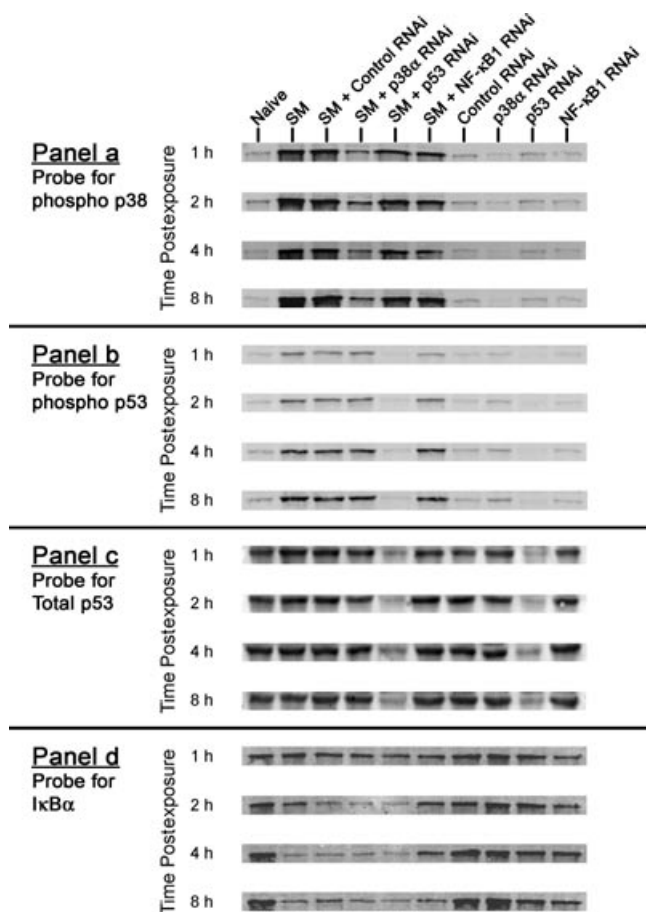
FIGURE 5. Western blot analyses of p38 phosphorylation (panel a), p53 phosphorylation (panel b), total p53 (panel c), and IκBα (panel d) in SM-exposed NHEK. NHEK were treated with RNAi for 48 h and exposed to 200 μM SM for the indicated time. Whole cell lysates were prepared, resolved by SDS-PAGE, immunoblotted, and probed with antibodies for phospho p38 (threonine180/tyrosine182), phospho p53 (serine 15), total p53, or IκBα. The data shown are representative of three biological replicates.

observed in any of the unexposed RNAi-transfected groups (data not shown).

p38, p53, and NF-κB Signaling

The roles of p38, p53, and NF-κB in SM-induced signaling were also investigated by Western blot analysis. NHEK were treated with RNAi and exposed to 200 μM SM, and whole cell lysates were collected at 1, 2, 4, and 8 h after exposure. Samples were normalized by total protein content, then resolved and blotted. p38 phosphorylation appeared maximal at the earliest time point of 1 h, and there was no apparent increase over the 8-h time course (Figure 5, panel a). p38 phosphorylation was roughly equivalent among the SM-exposed experimental groups, with the exception of p38 RNAi-treated cells. SM exposure also induced the phosphorylation

of p53 (Figure 5, panel b). p53 phosphorylation was observable at 1 h, but increased over the 8-h time course. Phosphorylation of p53 was equivalent among the SM-exposed experimental groups at each time point with the exception of p53 RNAi-treated cells. We also evaluated activation of p53 by analyzing the accumulation of total p53. SM did not appear to induce the accumulation of p53 in NHEK (Figure 5, panel c), and the levels of p53 in NHEK appeared to be equivalent among both SM-exposed and unexposed groups at all time points; again with the exception of cells treated with p53 RNAi. Since degradation of IκBα occurs during the activation of NF-κB, we analyzed the degradation of IκBα as a surrogate marker of NF-κB activation (Figure 5, panel d). Unlike p53, which is activated early in SM-exposed cells, IκBα degradation was not apparent until 2 h after SM exposure. IκBα degradation was equivalent among the SM-exposed experimental groups at the 8-h time point. IκBα degradation was slightly less in SM-exposed NF-κB1 RNAi-treated cells at the 2- and 4-h time points relative to the other SM-exposed experimental groups.

DISCUSSION

p38 RNAi significantly inhibited the SM-induced production of IL-8, IL-6, and TNFα by NHEK. These findings are consistent with a previous report from our laboratory investigating p38 signaling in SM-exposed NHEK [7]. In that study, we used the p38 inhibitor SB203580 and demonstrated substantial and significant inhibition of inflammatory cytokine production (IL-1β, IL-6, IL-8, and TNFα) by SM-exposed NHEK. Taken together, these studies suggest that p38 may play a critical role in signaling inflammatory cytokine production in SM-exposed NHEK. p38 RNAi did not appear to affect SM-induced loss of membrane integrity or phenotypic changes, which suggests that p38 may not play a role in the fate of cells exposed to SM. p38 activation was apparent at our earliest time point analyzed, which was 1 h postexposure. This is consistent with previous reports that p38 is activated early in SM-exposed cells [7,11].

NF-κB1 RNAi (which targets the canonical NF-κB p50 subunit) did not inhibit the SM-induced production of IL-8, IL-6, and TNFα by NHEK, but rather increased the production of IL-6 and IL-8. One possibility for this observation is that since NF-κB1 RNAi-treated cells appear to be healthier slightly longer than SM-exposed cells, they may have a longer opportunity to produce cytokines. Alternatively, p50 or NF-κB plays a negative role in regulating these cytokines in SM injury. NF-κB1 RNAi, as well as p38 RNAi, inhibited SM-induced IL-1β production though not significantly. These findings suggest the possibility that NF-κB may

not play a major role in SM-induced inflammatory cytokine production by this cell type, with the exception of a partial role in IL-1β. This possibility may be supported by recent findings of Rebholz et al. [11] investigating the SM-induced activation of MAPK and NF-κB/RelA pathways in keratinocytes. Utilizing wild type and RelA-knockout cells, they showed by electrophoretic mobility-shift assays that only the canonical NF-κB pathway is activated by SM (no binding activity of p52, RelB, or c-Rel was observed). This activation was dependent on RelA and other NF-κB family members could not substitute in cells lacking RelA. Our observations with p50 RNAi suggest that other NF-κB family members, namely p52, may not be able to substitute for the role of p50 in the SM-induced NF-κB response. However, it is important to note that RelA may have activities that are independent of p50 [31,32]; therefore, future studies will be performed using RNAi to target RelA, as well as the noncanonical NF-κB family members p52, RelB, and c-Rel to further elucidate the role of NF-κB in SM-injury in our system. Our results do suggest a role for NF-κB in the fate of cells exposed to SM in that NF-κB1 RNAi moderately delays and diminishes SM-induced phenotypic changes and loss of membrane integrity. NF-κB may play a prodeath role given the trend toward improved cell viability with p50 inhibition. This would be consistent with reports of a correlation between decreased NF-κB activity and improved viability with SM-exposed cells [9,10,13]; however, firm comparisons to these previous reports are difficult due to broad activity of the inhibitors and therapeutics used in those studies.

Our results do not support a role for p53 in SM-induced inflammatory cytokine production. p53 has been implicated in the fate of cells exposed to SM [10,23,24,26,27]. Upregulation of p53 by HPV E7 was observed to sensitize cells to SM-induced death [23,25]. Considering these previous studies, we anticipated that p53 RNAi would attenuate SM-induced apoptosis in our system and result in improved markers of cell viability. Interestingly, p53 RNAi treatment had the opposite effect. However surprising these findings may be, they are not unprecedented. Chaturvedi et al. [33] also observed that p53 RNAi treatment of primary human keratinocytes enhanced cell death in their model of UV light-induced apoptosis. The authors suggested that the vulnerability of p53 RNAi-treated cells may be due to a reduced capacity for DNA repair; if cells cannot efficiently repair their damaged DNA, they will more rapidly progress to apoptosis. Adding to the difficulty of understanding the role of p53 in the fate of cells exposed to SM is the caveat that there may not be a simple relationship between cellular levels of p53 and apoptotic responses [34,35]. While the effects of p53 RNAi inhibition by RNAi were surprising, the kinetics

of p53 activation was not. We observed p53 activation at our earliest time point analyzed which was 1 h postexposure. This is consistent with previous reports that p53 is activated early in SM-exposed cells [7,10,11,24]. We did not observe accumulation of p53 in SM-exposed NHEK, which can occur since p53 is a positive regulator of its own transcription [4].

Several studies have shown crosstalk between the p38, p53, and NF-κB pathways in other systems [36–40]. Any potential crosstalk between these pathways in SM-exposed cells would be relevant in understanding the molecular mechanisms of SM-induced injury. Our Western blot analyses show that RNAi inhibition of any one of these molecules does not ultimately affect the SM-induced activation of any of the others. These results suggest that there may be no crosstalk between these pathways in SM-induced signaling or that any crosstalk that may occur is downstream of these molecules. These observations are similar to those recently reported by Rebholz et al. [11]. They observed that SM-induced activation of the p38 pathway was no different in RelA-deficient and wild type cells indicating that NF-κB signaling in SM exposure was independent of p38 signaling. The apparent lack of crosstalk between these molecules in their system is consistent with our observations that RNAi against each of these molecules each had very different effects on SM-exposed cells: (1) p38 inhibition attenuates inflammatory cytokine production, (2) NF-κB inhibition modestly improves markers of cell viability, and (3) p53 inhibition accelerates and potentiates cell death.

This is the first report suggesting that NF-κB may not play a primary role in the inflammatory response of SM-exposed cells. Furthermore, a primary role for p38 in SM-induced cytokine production has now been demonstrated using two different approaches; RNAi and SB203580. These findings have important implications for future research given that NF-κB has long been implicated as playing a primary role in SM-induced inflammatory cytokine production [9,12–14]. Similarly, p53 is widely believed to play a prodeath role in SM-exposed cells [10,23,24,26,27]. However, our findings with p53 RNAi demonstrate the complexities of understanding the role of this molecule in the fate of cells exposed to SM. Given that p38, NF-κB, and p53 have been implicated as important pathways involved in the cellular response to SM, our findings provide relevant direction for future SM research.

SUPPLEMENTARY DATA

A supplement to Figure 4 showing panel c:24 h postexposure is available from the corresponding author on request.

ACKNOWLEDGMENTS

REFERENCES

1. Papirmeister B, Feister A, Robinson S, Ford R. Medical defense against mustard gas: Toxic mechanisms and pharmacological implications. Boca Raton, FL: CRC Press; 1991.
2. Chang L, Karin M. Mammalian MAP kinase signalling cascades. Nature 2001;410(6824):37–40.
3. Cuenda A, Rousseau S. p38 MAP-kinases pathway regulation, function and role in human diseases. Biochim Biophys Acta 2007;1773(8):1358–1375.
4. Gomez-Lazaro M, Fernandez-Gomez FJ, Jordan J. p53: twenty five years understanding the mechanism of genome protection. J Physiol Biochem 2004;60(4):287–307.
5. Chen LF, Greene WC. Shaping the nuclear action of NF-κB. Nat Rev Mol Cell Biol 2004;5(5):392–401.
6. Arroyo CM, Kan RK, Burman DL, Kahler DW, Nelson MR, Corun CM, Guzman JJ, Broomfield CA. Regulation of 1-α,25-dihydroxyvitamin D3 on interleukin-6 and interleukin-8 induced by sulfur mustard (HD) on human skin cells. Pharmacol Toxicol 2003;92(5):204–213.
7. Dillman JF, III, McGary KL, Schlager JJ. An inhibitor of p38 MAP kinase downregulates cytokine release induced by sulfur mustard exposure in human epidermal keratinocytes. Toxicol In Vitro 2004;18(5):593–599.
8. Sabourin CL, Petrali JP, Casillas RP. Alterations in inflammatory cytokine gene expression in sulfur mustard-exposed mouse skin. J Biochem Mol Toxicol 2000;14(6):291–302.
9. Atkins KB, Lodhi IJ, Hurley LL, Hinshaw DB. N-Acetylcysteine and endothelial cell injury by sulfur mustard. J Appl Toxicol 2000;20(Suppl 1):S125–S128.
10. Minsavage GD, Dillman JF, III. Bifunctional alkylating agent-induced p53 and nonclassical nuclear factor κB responses and cell death are altered by caffeic acid phenethyl ester: a potential role for antioxidant/electrophilic response-element signaling. J Pharmacol Exp Ther 2007;321(1):202–212.
11. Rebholz B, Kehe K, Ruzicka T, Rupec RA. Role of NF-κB/RelA and MAPK pathways in keratinocytes in response to sulfur mustard. J Invest Dermatol 2008;128(7):1626–1632.
12. Chatterjee D, Mukherjee S, Smith MG, Das SK. Signal transduction events in lung injury induced by 2-chloroethyl ethyl sulfide, a mustard analog. J Biochem Mol Toxicol 2003;17(2):114–121.
13. Das SK, Mukherjee S, Smith MG, Chatterjee D. Prophylactic protection by N-acetylcysteine against the pulmonary injury induced by 2-chloroethyl ethyl sulfide, a mustard analogue. J Biochem Mol Toxicol 2003;17(3):177–184.
14. Qabar A, Nelson M, Guzman J, Corun C, Hwang BJ, Steinberg M. Modulation of sulfur mustard induced cell death in human epidermal keratinocytes using IL-10 and TNF-α. J Biochem Mol Toxicol 2005;19(4):213–225.
15. Baeuerle PA, Henkel T. Function and activation of NF-κB in the immune system. Annu Rev Immunol 1994;12:141–179.
16. Christman JW, Sadikot RT, Blackwell TS. The role of nuclear factor-κB in pulmonary diseases. Chest 2000;117(5):1482–1487.
17. Ginzler AM, Davis MI. The pathology of mustard burns of human skin. Edgewood Arsenal, MD: U.S. Army Medical Research Laboratory; 1943. Report nr MRL (EA) 3.
18. Henriques FC, Moritz AR, Breyfogle HS, Patterson LA. The mechanism of cutaneous injury by mustard gas. An experimental study using mustard prepared with radioactive sulfur: Harvard University; 1944 5/9/44. Report nr OSRD 3653.
19. Beg AA, Baltimore D. An essential role for NF-κB in preventing TNF-α-induced cell death. Science 1996;274(5288):782–784.
20. Plumpe J, Malek NP, Bock CT, Rakemann T, Manns MP, Trautwein C. NF-κB determines between apoptosis and proliferation in hepatocytes during liver regeneration. Am J Physiol Gastrointest Liver Physiol 2000;278(1):G173–G183.
21. Shang J, Eberle J, Geilen CC, Hossini AM, Fecker LF, Orfanos CE, Tebbe B. The role of nuclear factor-κB and melanogenesis in tumor necrosis factor-alpha-induced apoptosis of normal human melanocytes. Skin Pharmacol Appl Skin Physiol 2002;15(5):321–329.
22. Xu Y, Bialik S, Jones BE, Iimuro Y, Kitsis RN, Srinivasan A, Brenner DA, Czaja MJ. NF-κB inactivation converts a hepatocyte cell line TNF-α response from proliferation to apoptosis. Am J Physiol 1998;275(4 Pt 1):C1058–C1066.
23. Rosenthal DS, Simbulan-Rosenthal CM, Iyer S, Smith WJ, Ray R, Smulson ME. Calmodulin, poly(ADP-ribose)polymerase and p53 are targets for modulating the effects of sulfur mustard. J Appl Toxicol 2000;20(Suppl 1):S43–S49.
24. Rosenthal DS, Simbulan-Rosenthal CM, Iyer S, Spoonde A, Smith W, Ray R, Smulson ME. Sulfur mustard induces markers of terminal differentiation and apoptosis in keratinocytes via a Ca^{2+}-calmodulin and caspase-dependent pathway. J Invest Dermatol 1998;111(1):64–71.
25. Stoppler H, Stoppler MC, Johnson E, Simbulan-Rosenthal CM, Smulson ME, Iyer S, Rosenthal DS, Schlegel R. The E7 protein of human papillomavirus type 16 sensitizes primary human keratinocytes to apoptosis. Oncogene 1998;17(10):1207–1214.
26. Dillman JF, III, Phillips CS, Dorsch LM, Croxton MD, Hege AI, Sylvester AJ, Moran TS, Sciuto AM. Genomic analysis of rodent pulmonary tissue following bis-(2-chloroethyl) sulfide exposure. Chem Res Toxicol 2005;18(1):28–34.
27. Smith KJ, Graham JS, Hamilton TA, Skelton HG, Petrali JP, Hurst CG. Immunohistochemical studies of basement membrane proteins and proliferation and apoptosis markers in sulfur mustard induced cutaneous lesions in weanling pigs. J Dermatol Sci 1997;15(3):173–182.
28. Decker T, Lohmann-Matthes ML. A quick and simple method for the quantitation of lactate dehydrogenase release in measurements of cellular cytotoxicity and tumor necrosis factor (TNF) activity. J Immunol Methods 1988;115(1):61–69.
29. Korzeniewski C, Callewaert DM. An enzyme-release assay for natural cytotoxicity. J Immunol Methods 1983;64(3):313–320.

30. Beardmore VA, Hinton HJ, Eftychi C, Apostolaki M, Armaka M, Darragh J, McIlrath J, Carr JM, Armit LJ, Clacher C, Malone L, Kollias G, Arthur JSC. Generation and characterization of p38beta (MAPK11) gene-targeted mice. Mol Cell Biol 2005;25(23):10454–10464.

31. Kato A, Edwards MJ, Lentsch AB. Gene deletion of NF-κB p50 does not alter the hepatic inflammatory response to ischemia/reperfusion. J Hepatol 2002;37(1): 48–55.

32. Gomez PF, Pillinger MH, Attur M, Marjanovic N, Dave M, Park J, Bingham CO, III, Al-Mussawir H, Abramson SB. Resolution of inflammation: prostaglandin E2 dissociates nuclear trafficking of individual NF-κB subunits (p65, p50) in stimulated rheumatoid synovial fibroblasts. J Immunol 2005;175(10):6924–6930.

33. Chaturvedi V, Sitailo LA, Qin JZ, Bodner B, Denning MF, Curry J, Zhang W, Brash D, Nickoloff BJ. Knockdown of p53 levels in human keratinocytes accelerates Mcl-1 and Bcl-x(L) reduction thereby enhancing UV-light induced apoptosis. Oncogene 2005;24(34): 5299–5312.

34. Greenhalgh DA, Wang XJ, Donehower LA, Roop DR. Paradoxical tumor inhibitory effect of p53 loss in transgenic mice expressing epidermal-targeted v-rasHa, v-fos, or human transforming growth factor alpha. Cancer Res 1996;56(19):4413–4423.

35. Jiang W, Ananthaswamy HN, Muller HK, Kripke ML. p53 protects against skin cancer induction by UV-B radiation. Oncogene 1999;18(29):4247–4253.

36. Bohuslav J, Chen LF, Kwon H, Mu Y, Greene WC. p53 induces NF-κB activation by an IκB kinase-independent mechanism involving phosphorylation of p65 by ribosomal S6 kinase 1. J Biol Chem 2004;279(25):26115–26125.

37. Fujioka S, Schmidt C, Sclabas GM, Li Z, Pelicano H, Peng B, Yao A, Niu J, Zhang W, Evans DB, Abbruzzese JL, Huang P, Chiao PJ. Stabilization of p53 is a novel mechanism for proapoptotic function of NF-κB. J Biol Chem 2004;279(26):27549–27559.

38. Jackson MW, Patt LE, LaRusch GA, Donner DB, Stark GR, Mayo LD. Hdm2 nuclear export, regulated by insulin-like growth factor-I/MAPK/p90Rsk signaling, mediates the transformation of human cells. J Biol Chem 2006;281(24):16814–16820.

39. Ryer EJ, Sakakibara K, Wang C, Sarkar D, Fisher PB, Faries PL, Kent KC, Liu B. Protein kinase C delta induces apoptosis of vascular smooth muscle cells through induction of the tumor suppressor p53 by both p38-dependent and p38-independent mechanisms. J Biol Chem 2005;280(42):35310–35317.

40. Webster GA, Perkins ND. Transcriptional cross talk between NF-κB and p53. Mol Cell Biol 1999;19(5):3485–3495.